OXFORD

an introduction to

nonlinear finite element analysis

J. N. REDDY

case, we begin with an assumed displacement field and compute strains that are consistent with the kinematic assumptions of the theory. Then we develop the weak forms using the principle of virtual displacements and the associated displacement finite element model. We also discuss certain computational aspects (e.g. membrane and shear locking) and iterative methods for the problems at hand. Computer implementation issues are also presented. Discussion of other linear finite element models of the Timoshenko beam theory are also presented for completeness.

4.2 Euler–Bernoulli Beams

4.2.1 Basic Assumptions

For the sake of completeness, the governing equations of the nonlinear bending of beams are developed from basic considerations. The classical beam theory is based on the Euler–Bernoulli hypothesis that plane sections perpendicular to the axis of the beam before deformation remain (a) plane, (b) rigid (not deform), and (c) rotate such that they remain perpendicular to the (deformed) axis after deformation. The assumptions amount to neglecting the Poisson effect and transverse strains. A refined theory is that due to Timoshenko, and it will be discussed in the sequel. The principle of virtual displacements will be used to formulate the variational problem and associated finite element model.

4.2.2 Displacement Field and Strains

The bending of beams with moderately large rotations but with small strains can be derived using the displacement field

$$u_1 = u_0(x) - z\frac{dw_0}{dx}, \quad u_2 = 0, \quad u_3 = w_0(x) \tag{4.2.1}$$

where (u_1, u_2, u_3) are the total displacements along the coordinate directions (x, y, z), and u_0 and w_0 denote the axial and transverse displacements of a point on the neutral axis.

Using the nonlinear strain-displacement relations (sum on repeated subscripts is implied; see Chapter 9)

$$\varepsilon_{ij} = \frac{1}{2}\left(\frac{\partial u_i}{\partial x_j} + \frac{\partial u_j}{\partial x_i}\right) + \frac{1}{2}\left(\frac{\partial u_m}{\partial x_i}\frac{\partial u_m}{\partial x_j}\right) \tag{4.2.2}$$

and omitting the large strain terms but retaining only the square of du_3/dx (which represents the rotation of a transverse normal line in the beam), we obtain

$$\begin{aligned}\varepsilon_{11} = \varepsilon_{xx} &= \frac{du_0}{dx} - z\frac{d^2w_0}{dx^2} + \frac{1}{2}\left(\frac{dw_0}{dx}\right)^2 \\ &= \left[\frac{du_0}{dx} + \frac{1}{2}\left(\frac{dw_0}{dx}\right)^2\right] - z\left(\frac{d^2w_0}{dx^2}\right) \\ &\equiv \varepsilon^0_{xx} + z\varepsilon^1_{xx} \end{aligned} \tag{4.2.3a}$$

$$\varepsilon^0_{xx} = \frac{du_0}{dx} + \frac{1}{2}\left(\frac{dw_0}{dx}\right)^2, \quad \varepsilon^1_{xx} = -\frac{d^2w_0}{dx^2} \tag{4.2.3b}$$

and all other strains are zero. Note that the notation $x_1 = x$, $x_2 = y$, and $x_3 = z$ is used. These strains are known as the *von Kármán strains*.

4.2.3 Weak Forms

The weak form of structural problems can be directly derived (i.e. without knowing the governing differential equations) using the principle of virtual displacements. The principle states that *if a body is in equilibrium, the total virtual work done by actual internal as well as external forces in moving through their respective virtual displacements is zero.* The virtual displacements are arbitrary except that they are zero where displacements are prescribed. The analytical form of the principle over a typical element $\Omega^e = (x_a, x_b)$ (see Figure 4.2.1) is given by (see Reddy [2])

$$\delta W^e \equiv \delta W^e_I - \delta W^e_E = 0 \tag{4.2.4}$$

where δW^e_I is the virtual strain energy stored in the element due to actual stresses σ_{ij} in moving through the virtual strains $\delta\varepsilon_{ij}$, and δW^e_E is the work done by externally applied loads in moving through their respective virtual displacements. Here σ_{ij} and ε_{ij} denote the Cartesian components of the stress and the Green strain tensors, respectively. Due to the assumption of small strains, no distinction will be made here between the Cauchy and second Piola–Kirchhoff stress tensors (see Chapter 9).

For the beam element, we have

$$\begin{aligned}\delta W^e_I &= \int_{V^e} \delta\varepsilon_{ij}\,\sigma_{ij}\, dV \\ \delta W^e_E &= \int_{x_a}^{x_b} q\,\delta w_0\, dx + \int_{x_a}^{x_b} f\,\delta u_0\, dx + \sum_{i=1}^{6} Q^e_i\,\delta\Delta^e_i \end{aligned} \tag{4.2.5}$$

where V^e denotes the element volume, $q(x)$ is the distributed transverse load (measured per unit length), $f(x)$ is the distributed axial load (measured per unit length), Q^e_i are the generalized nodal forces, and $\delta\Delta^e_i$ are the virtual generalized nodal displacements of the element (see Figure 4.2.1) defined by

$$\Delta_1^e = u_0(x_a),\ \ \Delta_2^e = w_0(x_a),\ \ \Delta_3^e = \left[-\frac{dw_0}{dx}\right]_{x_a} \equiv \theta(x_a)$$
$$\Delta_4^e = u_0(x_b),\ \ \Delta_5^e = w_0(x_b),\ \ \Delta_6^e = \left[-\frac{dw_0}{dx}\right]_{x_b} \equiv \theta(x_b) \tag{4.2.6a}$$

$$Q_1^e = -N_{xx}(x_a),\quad Q_4^e = N_{xx}(x_b)$$
$$Q \neq V \equiv Q_2^e = -\left[\frac{dw_0}{dx}N_{xx} + \frac{dM_{xx}}{dx}\right]_{x_a},\quad Q_5^e = \left[\frac{dw_0}{dx}N_{xx} + \frac{dM_{xx}}{dx}\right]_{x_b}$$
$$Q_3^e = -M_{xx}(x_a),\quad Q_6^e = M_{xx}(x_b) \tag{4.2.6b}$$

In view of the explicit nature of the assumed displacement field (4.2.5) in the thickness coordinate z and its independence of coordinate y, the volume integral can be expressed as a product of integrals over the length and area of the element:

$$\int_{V^e} (\cdot)\, dV = \int_{x_a}^{x_b}\int_{A^e} (\cdot)\, dA\, dx$$

Therefore, the expression for the virtual strain energy can be simplified as follows (only non-zero components of strain and stress are $\varepsilon_{11} \equiv \varepsilon_{xx}$ and $\sigma_{11} \equiv \sigma_{xx}$)

$$\begin{aligned}\delta W_I^e &= \int_{x_a}^{x_b}\int_{A^e} \delta\varepsilon_{xx}\,\sigma_{xx}\, dA\, dx = \int_{x_a}^{x_b}\int_{A^e}\left(\delta\varepsilon_{xx}^0 + z\delta\varepsilon_{xx}^1\right)\sigma_{xx}\, dA\, dx\\ &= \int_{x_a}^{x_b}\int_{A^e}\left[\left(\frac{d\delta u_0}{dx} + \frac{dw_0}{dx}\frac{d\delta w_0}{dx}\right) - z\frac{d^2\delta w_0}{dx^2}\right]\sigma_{xx}\, dA\, dx\\ &= \int_{x_a}^{x_b}\left[\left(\frac{d\delta u_0}{dx} + \frac{dw_0}{dx}\frac{d\delta w_0}{dx}\right)N_{xx} - \frac{d^2\delta w_0}{dx^2}M_{xx}\right] dx\end{aligned} \tag{4.2.7}$$

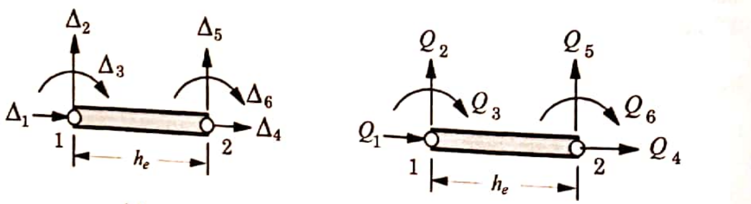

(a) (b)

Figure 4.2.1 The Euler–Bernoulli beam finite element with generalized displacement and force degrees of freedom. (a) Nodal displacements. (b) Nodal forces.

where N_{xx} is the axial force (measured per unit length) and M_{xx} is the moment (measured per unit length)

$$N_{xx} = \int_{A^e} \sigma_{xx}\, dA\,,\quad M_{xx} = \int_{A^e}\sigma_{xx} z\, dA \tag{4.2.8}$$

The virtual work statement in Eq. (4.2.7) becomes

$$\begin{aligned}0 = &\int_{x_a}^{x_b}\left[\left(\frac{d\delta u_0}{dx} + \frac{dw_0}{dx}\frac{d\delta w_0}{dx}\right)N_{xx} - \frac{d^2\delta w_0}{dx^2}M_{xx}\right] dx\\ &- \int_{x_a}^{x_b} q(x)\,\delta w_0(x)\, dx - \int_{x_a}^{x_b} f(x)\,\delta u_0(x)\, dx - \sum_{i=1}^{6} Q_i^e\,\delta\Delta_i^e\end{aligned} \tag{4.2.9}$$

The above weak form is equivalent to the following *two* statements, which are obtained by collecting terms involving δu_0 and δw_0 separately [see the definitions in Eqs. (4.2.6a,b)]:

$$0 = \int_{x_a}^{x_b}\left(\frac{d\delta u_0}{dx}N_{xx} - \delta u_0 f(x)\right) dx - Q_1^e\,\delta\Delta_1^e - Q_4^e\,\delta\Delta_4^e \tag{4.2.10a}$$

$$\begin{aligned}0 = &\int_{x_a}^{x_b}\left[\frac{d\delta w_0}{dx}\left(\frac{dw_0}{dx}N_{xx}\right) - \frac{d^2\delta w_0}{dx^2}M_{xx} - \delta w_0\, q(x)\right] dx\\ &- Q_2^e\,\delta\Delta_2^e - Q_3^e\,\delta\Delta_3^e - Q_5^e\,\delta\Delta_5^e - Q_6^e\,\delta\Delta_6^e\end{aligned} \tag{4.2.10b}$$

The differential equations governing nonlinear bending of straight beams can be obtained, although not needed for finite element model development, from the virtual work statement in (4.2.9), equivalently, the weak forms (4.2.10a,b), or from a vector approach in which forces and moments are summed over a typical beam element.

Integration by parts of the expressions in (4.2.9) to relieve δu_0 and δw_0 of any differentiation results in

$$\begin{aligned}0 = &\int_{x_a}^{x_b}\left\{\left(-\frac{dN_{xx}}{dx} - f\right)\delta u_0 - \left[\frac{d}{dx}\left(\frac{dw_0}{dx}N_{xx}\right) + \frac{d^2M_{xx}}{dx^2} + q\right]\delta w_0\right\} dx\\ &+ \left[N_{xx}\delta u_0 + \left(\frac{dw_0}{dx}N_{xx} + \frac{dM_{xx}}{dx}\right)\delta w_0 - M_{xx}\frac{d\delta w_0}{dx}\right]_{x_a}^{x_b} - \sum_{i=1}^{6} Q_i^e\,\delta\Delta_i^e\end{aligned}$$

Since δu_0 and δw_0 are arbitrary and independent of each other in $x_a < x < x_b$ as well as at $x = x_a$ and $x = x_b$ (independently), it follows that the governing equations of equilibrium, known as the Euler equations, are

$$\delta u_0: \quad -\frac{dN_{xx}}{dx} = f(x) \tag{4.2.11a}$$

$$\delta w_0: \quad -\frac{d}{dx}\left(\frac{dw_0}{dx}N_{xx}\right) - \frac{d^2M_{xx}}{dx^2} = q(x) \tag{4.2.11b}$$

In view of the definitions (4.2.6a), definitions (4.2.6b) are obtained as the natural (or force) boundary conditions

$$
\begin{aligned}
&Q_1^e + N_{xx}(x_a) = 0, \quad Q_4^e - N_{xx}(x_b) = 0\\
&Q_2^e + \left[\frac{dw_0}{dx}N_{xx} + \frac{dM_{xx}}{dx}\right]_{x_a} = 0, \quad Q_5^e - \left[\frac{dw_0}{dx}N_{xx} + \frac{dM_{xx}}{dx}\right]_{x_b} = 0\\
&Q_3^e + M_{xx}(x_a) = 0, \quad Q_6^e - M_{xx}(x_b) = 0
\end{aligned}
\tag{4.2.12}
$$

The vector approach involves identifying a typical beam element of length Δx with all its forces and moments, summing them, and taking the limit $\Delta x \to 0$. Consider the beam element shown in Figure 4.2.2, where N_{xx} is the internal axial force, $V(x)$ is the internal vertical shear force, M_{xx} is the internal bending moment, $f(x)$ is the external axial force, and $q(x)$ is external distributed transverse load. Summing the forces in the x and z coordinate directions, and moments about the y axis, we obtain

$$
\begin{aligned}
\sum F_x = 0: &\quad -N_{xx} + (N_{xx} + \Delta N_{xx}) + f(x)\Delta x = 0\\
\sum F_z = 0: &\quad -V + (V + \Delta V) + q(x)\Delta x = 0\\
\sum M_y = 0: &\quad -M_{xx} + (M_{xx} + \Delta M_{xx}) - V\Delta x + N_{xx}\Delta x\frac{dw_0}{dx}\\
&\quad + q(x)\Delta x(c\Delta x) = 0
\end{aligned}
$$

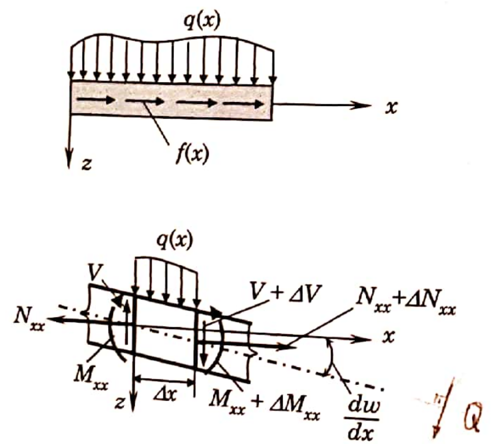

Figure 4.2.2 A typical beam element with forces and moments to derive equations of equilibrium using the vector approach.

Taking the limit $\Delta x \to 0$, we obtain the following three equations:

$$
\begin{aligned}
&\frac{dN_{xx}}{dx} + f(x) = 0\\
&\frac{dV}{dx} + q(x) = 0\\
&\frac{dM_{xx}}{dx} - V + N_{xx}\frac{dw_0}{dx} = 0
\end{aligned}
$$

$\frac{dM_{xx}}{dx} = Q$

which are equivalent to the two equations in (4.2.11a,b). Note that V is the shear force on a section perpendicular to the x-axis, and it is not equal to the shear force $Q(x)$ acting on the section perpendicular to the deformed beam. In fact, one can show that $V = Q + N_{xx}(dw_0/dx)$.

If one starts with the governing equations (4.2.11a,b), their weak forms can be developed using the usual three-step procedure:

$$
\begin{aligned}
0 &= \int_{x_a}^{x_b} v_1\left(-\frac{dN_{xx}}{dx} - f\right)dx\\
&= \int_{x_a}^{x_b}\left(\frac{dv_1}{dx}N_{xx} - v_1 f\right)dx - [v_1 N_{xx}]_{x_a}^{x_b}\\
&= \int_{x_a}^{x_b}\left(\frac{dv_1}{dx}N_{xx} - v_1 f\right)dx - v_1(x_a)[-N_{xx}(x_a)] - v_1(x_b)N_{xx}(x_b)
\end{aligned}
\tag{4.2.13a}
$$

$$
\begin{aligned}
0 &= \int_{x_a}^{x_b} v_2\left[-\frac{d}{dx}\left(\frac{dw_0}{dx}N_{xx}\right) - \frac{d^2M_{xx}}{dx^2} - q\right]dx\\
&= \int_{x_a}^{x_b}\left[\frac{dv_2}{dx}\left(\frac{dw_0}{dx}N_{xx}\right) - \frac{d^2v_2}{dx^2}M_{xx} - v_2 q\right]dx\\
&\quad - \left[v_2\left(\frac{dw_0}{dx}N_{xx} + \frac{dM_{xx}}{dx}\right)\right]_{x_a}^{x_b} - \left[\left(-\frac{dv_2}{dx}\right)M_{xx}\right]_{x_a}^{x_b}\\
&= \int_{x_a}^{x_b}\left[\frac{dv_2}{dx}\left(\frac{dw_0}{dx}N_{xx}\right) - \frac{d^2v_2}{dx^2}M_{xx} - v_2 q\right]dx\\
&\quad - v_2(x_a)\left[-\left(\frac{dw_0}{dx}N_{xx} - \frac{dM_{xx}}{dx}\right)\right]_{x_a} - v_2(x_b)\left[\frac{dw_0}{dx}N_{xx} + \frac{dM_{xx}}{dx}\right]_{x_b}\\
&\quad - \left[-\frac{dv_2}{dx}\right]_{x_a}[-M_{xx}(x_a)] - \left[-\frac{dv_2}{dx}\right]_{x_b}M_{xx}(x_b)
\end{aligned}
\tag{4.2.13b}
$$

where v_1 and v_2 are the weight functions, whose meaning is obvious if the expressions fv_1dx and qv_2dx are to represent the work done by external forces. We see that $v_1 \sim \delta u_0$ and $v_2 \sim \delta w_0$. Clearly, Eqs. (4.2.13a,b) are the same, with the definitions (4.2.6b) or (4.2.12), as those in Eqs. (4.2.10a,b).

The resultant force N_{xx} and moment M_{xx} can be expressed in terms of the displacements once the constitutive behavior is assumed. Suppose that the beam is made of a *linear elastic material*. Then the total stress is related to the total strain by Hooke's law

$$\sigma_{xx} = E^e \varepsilon_{xx} \tag{4.2.14}$$

Then we have

$$\begin{aligned} N_{xx} &= \int_{A^e} \sigma_{xx}\, dA = \int_{A^e} E^e \varepsilon_{xx}\, dA \\ &= \int_{A^e} E^e \left[\frac{du_0}{dx} + \frac{1}{2}\left(\frac{dw_0}{dx}\right)^2 - z\frac{d^2 w_0}{dx^2}\right] dA \\ &= A^e_{xx}\left[\frac{du_0}{dx} + \frac{1}{2}\left(\frac{dw_0}{dx}\right)^2\right] - B^e_{xx}\frac{d^2 w_0}{dx^2} \end{aligned} \tag{4.2.15a}$$

$$\begin{aligned} M_{xx} &= \int_{A^e} \sigma_{xx}\, z\, dA = \int_{A^e} E^e \varepsilon_{xx}\, z\, dA \\ &= \int_{A^e} E^e \left[\frac{du_0}{dx} + \frac{1}{2}\left(\frac{dw_0}{dx}\right)^2 - z\frac{d^2 w_0}{dx^2}\right] z\, dA \\ &= B^e_{xx}\left[\frac{du_0}{dx} + \frac{1}{2}\left(\frac{dw_0}{dx}\right)^2\right] - D^e_{xx}\frac{d^2 w_0}{dx^2} \end{aligned} \tag{4.2.15b}$$

where A^e_{xx}, B^e_{xx}, and D^e_{xx} are the extensional, extensional-bending, and bending stiffnesses of the beam element

$$(A^e_{xx},\ B^e_{xx},\ D^e_{xx}) = \int_{A^e} E^e \left(1, z, z^2\right) dA \tag{4.2.16}$$

For beams made of an isotropic material, the extensional–bending stiffness B^e_{xx} is zero when the x-axis is taken along the geometric centroidal axis. We have $B^e_{xx} = 0$, $A^e_{xx} = E^e A^e$, and $D^e_{xx} = E^e I^e$, where A^e and I^e are the cross-sectional area and second moment of inertia (about the y-axis) of the beam element. For simplicity, we shall omit the element label e on the variables. In general, A_{xx}, B_{xx}, and D_{xx} are functions of x whenever the modulus E and/or the cross-sectional area is a function of x.

The virtual work statements (4.2.10a,b) can be expressed in terms of the generalized displacements (u_0, w_0) by using Eqs. (4.2.15a,b). We have

$$\begin{aligned} 0 = \int_{x_a}^{x_b} A_{xx}\frac{d\delta u_0}{dx}\left[\frac{du_0}{dx} + \frac{1}{2}\left(\frac{dw_0}{dx}\right)^2\right] dx - \int_{x_a}^{x_b} f(x)\delta u_0\, dx \\ - Q_1\,\delta u_0(x_a) - Q_4\,\delta u_0(x_b) \end{aligned} \tag{4.2.17a}$$

$$\begin{aligned} 0 = \int_{x_a}^{x_b} \left\{ A_{xx}\frac{d\delta w_0}{dx}\frac{dw_0}{dx}\left[\frac{du_0}{dx} + \frac{1}{2}\left(\frac{dw_0}{dx}\right)^2\right] + D_{xx}\frac{d\delta^2 w_0}{dx^2}\frac{d^2 w_0}{dx^2}\right\} dx \\ - \int_{x_a}^{x_b} q\delta w_0\, dx - Q_2\,\delta w_0(x_a) - Q_3\,\delta\theta(x_a) - Q_5\,\delta w_0(x_b) - Q_6\,\delta\theta(x_b) \end{aligned} \tag{4.2.17b}$$

where it is assumed that the coupling coefficient B_{xx} is zero because of the choice of the coordinate system; that is, the x-axis is assumed to coincide with the geometric centroidal axis $\int_A z\, dA = 0$.

4.2.4 Finite Element Model

Let the axial displacement $u_0(x)$ and transverse deflection $w_0(x)$ are interpolated as $[\theta = -(dw_0/dx)]$

$$u_0(x) = \sum_{j=1}^{2} u_j \psi_j(x)\,, \quad w_0(x) = \sum_{j=1}^{4} \bar{\Delta}_j \phi_j(x) \tag{4.2.18}$$

$$\bar{\Delta}_1 \equiv w_0(x_a),\quad \bar{\Delta}_2 \equiv \theta(x_a),\quad \bar{\Delta}_3 \equiv w_0(x_b),\quad \bar{\Delta}_4 \equiv \theta(x_b) \tag{4.2.19}$$

and ψ_j are the linear Lagrange interpolation functions, and ϕ_j are the Hermite cubic interpolation functions. For a linear problem, this element gives exact nodal displacements u_i and $\bar{\Delta}_i$ for any $f(x)$ and $q(x)$ when A_{xx} and D_{xx} are element-wise constants. Then the element is said to be a *superconvergent* element.

Substituting Eq. (4.2.18) for $u_0(x)$, (4.2.19) for $w_0(x)$, and $\delta u_0(x) = \psi_i(x)$ and $\delta w_0(x) = \phi_i(x)$ (to obtain the ith algebraic equation of the model) into the weak forms (4.2.17a,b), we obtain

$$0 = \sum_{j=1}^{2} K^{11}_{ij} u_j + \sum_{J=1}^{4} K^{12}_{iJ}\bar{\Delta}_J - F^1_i \quad (i = 1, 2) \tag{4.2.20a}$$

$$0 = \sum_{j=1}^{2} K^{21}_{Ij} u_j + \sum_{J=1}^{4} K^{22}_{IJ}\bar{\Delta}_J - F^2_I \quad (I = 1, 2, 3, 4) \tag{4.2.20b}$$

where

$$\begin{aligned} K^{11}_{ij} &= \int_{x_a}^{x_b} A_{xx}\frac{d\psi_i}{dx}\frac{d\psi_j}{dx}\, dx\,, \quad K^{12}_{iJ} = \frac{1}{2}\int_{x_a}^{x_b}\left(A_{xx}\frac{dw_0}{dx}\right)\frac{d\psi_i}{dx}\frac{d\phi_J}{dx}\, dx \\ K^{21}_{Ij} &= \int_{x_a}^{x_b} A_{xx}\frac{dw_0}{dx}\frac{d\phi_I}{dx}\frac{d\psi_j}{dx}\, dx\,, \quad K^{21}_{Ij} = 2K^{12}_{jI} \\ K^{22}_{IJ} &= \int_{x_a}^{x_b} D_{xx}\frac{d^2\phi_I}{dx^2}\frac{d^2\phi_J}{dx^2}\, dx + \frac{1}{2}\int_{x_a}^{x_b}\left[A_{xx}\left(\frac{dw_0}{dx}\right)^2\right]\frac{d\phi_I}{dx}\frac{d\phi_J}{dx} dx \\ F^1_i &= \int_{x_a}^{x_b} f\,\psi_i\, dx + \hat{Q}_i\,, \quad F^2_I = \int_{x_a}^{x_b} q\,\phi_I\, dx + \bar{Q}_I \end{aligned} \tag{4.2.21}$$

for $(i, j = 1, 2)$ and $(I, J = 1, 2, 3, 4)$, where $\hat{Q}_1 = Q_1$, $\hat{Q}_2 = Q_4$, $\bar{Q}_1 = Q_2$, $\bar{Q}_2 = Q_3$, $\bar{Q}_3 = Q_5$, and $\bar{Q}_4 = Q_6$. See Eq. (4.2.6b) for the definitions of Q_i. Note that the coefficient matrices $[K^{12}], [K^{21}]$ and $[K^{22}]$ are functions of the unknown $w_0(x)$. Also, note that $[K^{12}]^T \neq [K^{21}]$; hence, the element direct stiffness matrix is unsymmetric.

The above definition of coefficients $K_{ij}^{\alpha\beta}$ is based on a particular linearization of Eqs. (4.2.17a,b), which is probably the most natural. Other forms of linearization are possible. For example, if consider Eq. (4.2.17a), the coefficient of $d\delta u_0/dx$ contains a linear term and a nonlinear term. To preserve the linear bar stiffness, the linear term should be kept as a part of the stiffness matrix. The nonlinear term can be either included in the stiffness coefficient, as is done in the definition given in Eq. (4.2.21), or the whole nonlinear term may be assumed to be known from the previous iteration. In the latter case, the term ends up in the load vector $\{F^1\}$. This choice of linearization is known to slow down the convergence. In the case of Eq. (4.2.17b), we know that the term dw_0/dx outside the square brackets is due to the nonlinear strain. Hence, it was linearized (i.e. calculated using the solution from the previous iteration) in defining K_{ij}^{21} of Eq. (4.2.21). One may linearize Eq. (4.2.17b) such that $du_0/dx + 0.5(dw_0/dx)^2$ is calculated using the solution from the previous iteration. In that case $K_{ij}^{21} = 0$ and K_{ij}^{22} will have additional contribution. Thus, it is possible to computationally decouple the equations for $\{u\}$ and $\{\bar{\Delta}\}$ and solve the two equations iteratively, feeding the solution from one equation to the other. However, such a strategy often results in nonconvergence.

Equations (4.2.20a,b) can be written compactly as

$$\sum_{\gamma=1}^{2}\sum_{p=1} K_{ip}^{\alpha\gamma}\Delta_p^\gamma = F_i^\alpha, \quad \text{or} \quad \sum_{p=1}^{2} K_{ip}^{\alpha 1} u_p + \sum_{P=1}^{4} K_{iP}^{\alpha 2}\bar{\Delta}_P = F_i^\alpha \tag{4.2.22}$$

In matrix form, we have

$$\begin{bmatrix} [K^{11}] & [K^{12}] \\ [K^{21}] & [K^{22}] \end{bmatrix} \begin{Bmatrix} \{\Delta^1\} \\ \{\Delta^2\} \end{Bmatrix} = \begin{Bmatrix} \{F^1\} \\ \{F^2\} \end{Bmatrix} \tag{4.2.23}$$

where

$$\Delta_i^1 = u_i, \quad i = 1,2; \quad \Delta_i^2 = \bar{\Delta}_i, \quad i = 1,2,3,4 \tag{4.2.24}$$

Note that the direct stiffness matrix is unsymmetric only due to the fact that $[K^{12}]$ contains the factor 1/2 whereas $[K^{21}]$ does not. One way to make $[K^{21}]^T = [K^{12}]$ is to split the linear strain du_0/dx in Eq. (4.2.17) into two equal parts and take one of the two parts as known from a previous iteration:

$$\begin{aligned} &\int_{x_a}^{x_b} \left\{ A_{xx}^e \frac{d\delta w_0}{dx}\frac{dw_0}{dx}\left[\frac{du_0}{dx} + \frac{1}{2}\left(\frac{dw_0}{dx}\right)^2\right]\right\} dx \\ &= \frac{1}{2}\int_{x_a}^{x_b} A_{xx}^e \left\{ \frac{dw_0}{dx}\frac{d\delta w_0}{dx}\frac{du_0}{dx} + \left[\frac{du_0}{dx} + \left(\frac{dw_0}{dx}\right)^2\right]\frac{d\delta w_0}{dx}\frac{dw_0}{dx}\right\} dx \end{aligned} \tag{4.2.25}$$

The first term of the above equation constitutes $[K^{21}]$ and the second one constitutes a part of $[K^{22}]$. The symmetrized equations are

$$\begin{bmatrix} [\bar{K}^{11}] & [\bar{K}^{12}] \\ [\bar{K}^{21}] & [\bar{K}^{22}] \end{bmatrix} \begin{Bmatrix} \{u\} \\ \{\bar{\Delta}\} \end{Bmatrix} = \begin{Bmatrix} \{F^1\} \\ \{F^2\} \end{Bmatrix} \tag{4.2.26}$$

where

$$\begin{aligned} \bar{K}_{ij}^{11} &= K_{ij}^{11} = \int_{x_a}^{x_b} A_{xx}^e \frac{d\psi_i}{dx}\frac{d\psi_j}{dx}\, dx \\ \bar{K}_{iJ}^{12} &= K_{iJ}^{12} = \frac{1}{2}\int_{x_a}^{x_b}\left(A_{xx}^e \frac{dw_0}{dx}\right)\frac{d\psi_i}{dx}\frac{d\phi_J}{dx}\, dx \\ \bar{K}_{Ij}^{21} &= \frac{1}{2}\int_{x_a}^{x_b}\left(A_{xx}^e \frac{dw_0}{dx}\right)\frac{d\phi_I}{dx}\frac{d\psi_j}{dx}\, dx\,, \quad \bar{K}_{Ij}^{21} = \bar{K}_{jI}^{12} \\ \bar{K}_{IJ}^{22} &= \int_{x_a}^{x_b} D_{xx}^e \frac{d^2\phi_I}{dx^2}\frac{d^2\phi_J}{dx^2}\, dx \\ &\quad + \frac{1}{2}\int_{x_a}^{x_b} A_{xx}^e \left[\frac{du_0}{dx} + \left(\frac{dw_0}{dx}\right)^2\right]\frac{d\phi_I}{dx}\frac{d\phi_J}{dx}\, dx \end{aligned} \tag{4.2.27}$$

Note that in the symmetrized case, we must assume that $u_0(x)$ is also known from a previous iteration.

4.2.5 Iterative Solutions of Nonlinear Equations

The direct iteration and Newton–Raphson methods introduced in Chapter 3 are revisited here in connection with the nonlinear finite element equations of the EBT. Consider the nonlinear equations (4.2.23), which can be written as

$$[K^e(\{\Delta^e\})]\{\Delta^e\} = \{F^e\} \tag{4.2.28}$$

where

$$\Delta_1^e = u_1,\ \Delta_2^e = \bar{\Delta}_1^e,\ \Delta_3^e = \bar{\Delta}_2^e,\ \Delta_4^e = u_2,\ \Delta_5^e = \bar{\Delta}_3^e\,,\ \Delta_6^e = \bar{\Delta}_4^e \tag{4.2.29a}$$

$$F_1^e = F_1^1,\ F_2^e = F_1^2,\ F_3^e = F_2^2,\ F_4^e = F_2^1,\ F_5^e = F_3^2,\ F_6^e = F_4^2 \tag{4.2.29b}$$

The system (4.2.28) of nonlinear algebraic equations can be linearized using the direct iteration and Newton–Raphson iterative methods of Section 3.4. These are presented next. Note that the linearized equations may be symmetric or unsymmetric, depending on the formulation, and therefore an appropriate equation solver must be used. On the other hand, an unsymmetric banded equations solver may be used in all cases.

Direct iteration procedure

In the direct iteration procedure, the solution at the rth iteration is determined from the assembled set of equations

$$[K(\{\Delta\}^{(r-1)})]\{\Delta\}^r = \{F\} \quad \text{or} \quad [\bar{K}(\{\Delta\}^{(r-1)})]\{\Delta\}^r = \{F\} \tag{4.2.30}$$

where the direct stiffness matrix $[K^e]$ is evaluated at the element level using the known solution $\{\Delta^e\}^{(r-1)}$ at the $(r-1)$st iteration.

Newton–Raphson iteration procedure

In the Newton-Raphson procedure, the linearized element equation is of the form

$$[T(\{\Delta\}^{(r-1)}][\Delta\}^r = -\{R(\{\Delta\}^{(r-1)})\} = \{F\} - ([K^e]\{\Delta^e\})^{(r-1)} \tag{4.2.31}$$

where the tangent stiffness matrix $[T^e]$ associated with the Euler–Bernoulli beam element is calculated using the definition

$$[T] \equiv \left(\frac{\partial\{R\}}{\partial\{\Delta\}}\right)^{(r-1)}, \quad \text{or} \quad T^e_{ij} \equiv \left(\frac{\partial R^e_i}{\partial \Delta^e_j}\right)^{(r-1)} \tag{4.2.32}$$

The solution at the rth iteration is then given by

$$\{\Delta\}^r = \{\Delta\}^{(r-1)} + \{\delta\Delta\} \tag{4.2.33}$$

Although the direct stiffness matrix $[K^e]$ is unsymmetric, it can be shown that the tangent stiffness matrix $[T^e]$ is symmetric. Further, it can be shown that the tangent stiffness matrix is the same whether one uses $[K^e]$ or $[\bar{K}^e]$ [see Eqs. (4.2.23) and (4.2.26)].

The coefficients of the element tangent stiffness matrix $[T^e]$ can be computed using the definition in (4.2.32). In terms of the components defined in Eq. (4.2.22), we can write

$$T^{\alpha\beta}_{ij} = \left(\frac{\partial R^\alpha_i}{\partial \Delta^\beta_j}\right)^{(r-1)} \tag{4.2.34}$$

for $\alpha, \beta = 1, 2$. The components of the residual vector can be expressed as

$$\begin{aligned} R^\alpha_i &= \sum_{\gamma=1}^{2}\sum_{p=1} K^{\alpha\gamma}_{ip}\Delta^\gamma_p - F^\alpha_i \\ &= \sum_{p=1}^{2} K^{\alpha 1}_{ip}\Delta^1_p + \sum_{P=1}^{4} K^{\alpha 2}_{iP}\Delta^2_P - F^\alpha_i \\ &= \sum_{p=1}^{2} K^{\alpha 1}_{ip} u_p + \sum_{P=1}^{4} K^{\alpha 2}_{iP}\bar{\Delta}_P - F^\alpha_i \end{aligned} \tag{4.2.35}$$

Note that the range of p is dictated by the size of the matrix $[K^{\alpha\beta}]$. We have

$$\begin{aligned} T^{\alpha\beta}_{ij} &= \left(\frac{\partial R^\alpha_i}{\partial \Delta^\beta_j}\right) = \frac{\partial}{\partial \Delta^\beta_j}\left(\sum_{\gamma=1}^{2}\sum_{p=1} K^{\alpha\gamma}_{ip}\Delta^\gamma_p - F^\alpha_i\right) \\ &= \sum_{\gamma=1}^{2}\sum_{p=1}\left(K^{\alpha\gamma}_{ip}\frac{\partial \Delta^\gamma_p}{\partial \Delta^\beta_j} + \frac{\partial K^{\alpha\gamma}_{ip}}{\partial \Delta^\beta_j}\Delta^\gamma_p\right) \\ &= K^{\alpha\beta}_{ij} + \sum_{p=1}^{2}\frac{\partial}{\partial \Delta^\beta_j}\left(K^{\alpha 1}_{ip}\right)u_p + \sum_{P=1}^{4}\frac{\partial}{\partial \Delta^\beta_j}\left(K^{\alpha 2}_{iP}\right)\bar{\Delta}_P \end{aligned} \tag{4.2.36}$$

We compute the tangent stiffness matrix coefficients $T^{\alpha\beta}_{ij}$ explicitly as shown below:

$$\begin{aligned} T^{11}_{ij} &= K^{11}_{ij} + \sum_{p=1}^{2}\frac{\partial K^{11}_{ip}}{\partial u_j}u_p + \sum_{P=1}^{4}\frac{\partial K^{12}_{iP}}{\partial u_j}\bar{\Delta}_P \\ &= K^{11}_{ij} + \sum_{p=1}^{2} 0\cdot u_p + \sum_{P=1}^{4} 0\cdot\bar{\Delta}_P \end{aligned} \tag{4.2.37}$$

Since

$$\frac{\partial K^{\alpha\beta}_{ij}}{\partial u_k} = 0 \text{ for all } \alpha, \beta, i, j \text{ and } k \tag{4.2.38}$$

the coefficients $[T^{11}]$ and $[T^{21}]$ of the tangent stiffness matrix are the same as those of the direct stiffness matrix:

$$[T^{11}] = [K^{11}] \ , \quad [T^{21}] = [K^{21}] \tag{4.2.39}$$

Next consider

$$\begin{aligned} T^{12}_{iJ} &= K^{12}_{iJ} + \sum_{p=1}^{2}\left(\frac{\partial K^{11}_{ip}}{\partial \bar{\Delta}_J}\right)u_p + \sum_{P=1}^{4}\left(\frac{\partial K^{12}_{iP}}{\partial \bar{\Delta}_J}\right)\bar{\Delta}_P \\ &= K^{12}_{iJ} + 0 + \sum_{P=1}^{4}\left[\int_{x_a}^{x_b}\frac{1}{2}A_{xx}\frac{\partial}{\partial \bar{\Delta}_J}\left(\frac{dw_0}{dx}\right)\frac{d\psi_i}{dx}\frac{d\phi_P}{dx}\,dx\right]\bar{\Delta}_P \\ &= K^{12}_{iJ} + \sum_{P=1}^{4}\left[\int_{x_a}^{x_b}\frac{1}{2}A_{xx}\frac{\partial}{\partial \bar{\Delta}_J}\left(\sum_{K=1}^{4}\bar{\Delta}_K\frac{d\phi_K}{dx}\right)\frac{d\psi_i}{dx}\frac{d\phi_P}{dx}\,dx\right]\bar{\Delta}_P \\ &= K^{12}_{iJ} + \sum_{P=1}^{4}\left[\int_{x_a}^{x_b}\frac{1}{2}A_{xx}\frac{d\phi_J}{dx}\frac{d\psi_i}{dx}\frac{d\phi_P}{dx}\,dx\right]\bar{\Delta}_P \\ &= K^{12}_{iJ} + \int_{x_a}^{x_b}\frac{1}{2}A_{xx}\frac{d\psi_i}{dx}\frac{d\phi_J}{dx}\left(\sum_{P=1}^{4}\frac{d\phi_P}{dx}\bar{\Delta}_P\right)dx \end{aligned}$$

$$= K_{iJ}^{12} + \int_{x_a}^{x_b} \left(\frac{1}{2} A_{xx} \frac{dw_0}{dx}\right) \frac{d\psi_i}{dx}\frac{d\phi_J}{dx}\, dx$$
$$= K_{iJ}^{12} + K_{iJ}^{12} = 2K_{iJ}^{12} = K_{Ji}^{21} \tag{4.2.40}$$

$$T_{IJ}^{22} = K_{IJ}^{22} + \sum_{p=1}^{2} \left(\frac{\partial K_{Ip}^{21}}{\partial \bar{\Delta}_J}\right) u_p + \sum_{P=1}^{4} \left(\frac{\partial K_{IP}^{22}}{\partial \bar{\Delta}_J}\right) \bar{\Delta}_P$$
$$= K_{IJ}^{22} + \sum_{p=1}^{2} \left[\int_{x_a}^{x_b} A_{xx} \frac{\partial}{\partial \bar{\Delta}_J} \left(\sum_{K}^{4} \bar{\Delta}_K \frac{d\phi_K}{dx}\right) \frac{d\phi_I}{dx}\frac{d\psi_p}{dx}\, dx\right] u_p$$
$$+ \sum_{P=1}^{4} \left[\int_{x_a}^{x_b} \frac{1}{2} A_{xx} \frac{\partial}{\partial \bar{\Delta}_J} \left(\frac{dw_0}{dx}\right)^2 \frac{d\phi_I}{dx}\frac{d\phi_P}{dx}\, dx\right] \bar{\Delta}_P$$
$$= K_{IJ}^{22} + \int_{x_a}^{x_b} A_{xx} \frac{d\phi_I}{dx}\frac{d\phi_J}{dx} \left(\sum_{p=1}^{2} \frac{d\psi_p}{dx} u_p\right) dx$$
$$+ \int_{x_a}^{x_b} A_{xx} \left(\frac{dw_0}{dx}\right) \frac{d\phi_I}{dx}\frac{d\phi_J}{dx} \left(\sum_{P=1}^{4} \bar{\Delta}_P \frac{d\phi_P}{dx}\right) dx$$
$$= K_{IJ}^{22} + \int_{x_a}^{x_b} A_{xx} \left(\frac{du_0}{dx} + \frac{dw_0}{dx}\frac{dw_0}{dx}\right) \frac{d\phi_I}{dx}\frac{d\phi_J}{dx}\, dx \tag{4.2.41}$$

4.2.6 Load Increments

Examining the expression (4.2.15a) for the internal axial force N_{xx}, it is clear that the rotation of a transverse normal contributes to tensile component of N_{xx} irrespective of the sign of the load. As a result, the beam becomes increasingly stiff with an increase in load. Hence, for large loads the nonlinearity may be too large for the numerical scheme to yield convergent solution. Therefore, it is necessary to divide the total load F into several smaller load increments $\delta F_1, \delta F_2, \ldots, \delta F_N$ such that

$$F = \sum_{i=1}^{N} \delta F_i \tag{4.2.42}$$

For the first load step, the iterative procedure outlined earlier can be used to determine the deflection. If it does not converge within a reasonable number of iterations, it may be necessary to further reduce the load increment $F_1 = \delta F_1$. Once the solution for the first load increment is obtained, it is used as the initial "guess" vector for the next load $F_2 = \delta F_1 + \delta F_2$. This is continued until the total load is reached.

Another way to accelerate the convergence is to use a weighted average of the solutions from the last two iterations in evaluating the stiffness matrix at

the rth iteration:

$$\{\Delta^*\}_{r-1} = \gamma\{\Delta\}_{r-2} + (1-\gamma)\{\Delta\}_{r-1}, \qquad 0 \le \gamma \le 1 \tag{4.2.43}$$

where γ is called the acceleration parameter. A value of $\gamma = 0.5$ is suggested when the iterative scheme experiences convergence difficulty. Otherwise, one should use $\gamma = 0$.

4.2.7 Membrane Locking

For the linear case, the axial displacement u_0 is uncoupled from the bending deflection w_0, and they can be determined independently from the finite element models [see Eqs. (4.2.20a,b)]

$$[K^{11}]\{u\} = \{F^1\}, \quad K_{ij}^{11} = \int_{x_a}^{x_b} A_{xx}^e \frac{d\psi_i}{dx}\frac{d\psi_j}{dx}\, dx \tag{4.2.44}$$

$$[K^{22(L)}]\{\bar{\Delta}\} = \{F^2\}, \quad K_{IJ}^{22(L)} = \int_{x_a}^{x_b} D_{xx}^e \frac{d^2\phi_I}{dx^2}\frac{d^2\phi_J}{dx^2}\, dx \tag{4.2.45}$$

respectively. Here the superscript L signifies the linear stiffness coefficients. Under the assumptions of linearity, if a beam is subjected to only bending forces and no axial loads, then $u_0(x) = 0$ when u_0 is specified to be zero at (at least) one point. In other words, a hinged–hinged beam and a pinned–pinned beam (see Figures 4.2.3(a) and (b), respectively) will have the same deflection $w_0(x)$ under the same loads and $u_0(x) = 0$ for all x. However, this is not the case when the beam undergoes nonlinear bending. The coupling between u_0 and w_0 will cause the beam to undergo axial displacement even when there are no axial forces, and the solution (u_0, w_0) will be different for the two cases shown in Figure 4.2.3.

First, we note that the hinged–hinged beam does not have any end constraints on u_0. If the geometry, boundary conditions, and loading are symmetric about the center, then $u_0 = 0$ there. Consequently, the beam does not experience any axial strain, that is, $\varepsilon_{xx}^0 = 0$ (because the beam is free to slide on the rollers to accommodate transverse deflection). On the other hand, the pinned–pinned beam is constrained from axial movement at $x = 0$ and $x = L$. As a result, it will develop axial strain to accommodate the transverse deflection. The former beam will have larger transverse deflection than the latter, as the latter offers axial stiffness to stretching, and the axial stiffness increases with the load.

Thus, for a hinged–hinged beam, the element should experience no stretching:

$$\varepsilon_{xx}^0 \equiv \frac{du_0}{dx} + \frac{1}{2}\left(\frac{dw_0}{dx}\right)^2 = 0 \text{ (membrane strain)} \tag{4.2.46}$$

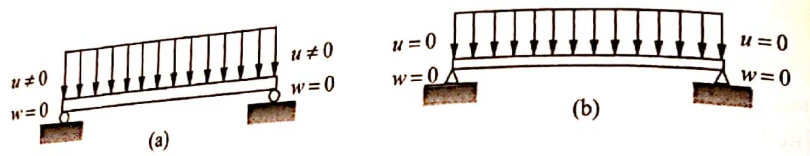

Figure 4.2.3 Nonlinear bending of (a) hinged–hinged and (b) pinned–pinned beams.

In order to satisfy the constraint in (4.2.46), we must have

$$\frac{du_0}{dx} \sim \left(\frac{dw_0}{dx}\right)^2 \tag{4.2.47}$$

The similarity is in the sense of having the same degree of polynomial variation of du_0/dx and $(dw_0/dx)^2$. For example, when u_0 is interpolated using linear functions and w_0 with cubic, the constraint in Eq. (4.2.47) is clearly *not* met and the resulting element stiffness matrix is excessively stiff (hence, results in zero displacement field), and the element is said to lock. This phenomenon is known as the *membrane locking*. In fact, unless a very higher-order interpolation of u_0 is used, the element will not satisfy the constraint.

A practical way to satisfy the constraint in Eq. (4.2.47) is to use the minimum interpolation of u_0 and w_0 (i.e. linear interpolation of u_0 and Hermite cubic interpolation of w_0) but treat ε_{xx}^0 as a constant. Since du_0/dx is constant, it is necessary to treat $(dw_0/dx)^2$ as a constant in numerically evaluating the element stiffness coefficients. Thus, if A_{xx} is a constant, all nonlinear stiffness coefficients should be evaluated using one-point Gauss quadrature, that is, use the *reduced integration*. These coefficients include K_{ij}^{12}, K_{ij}^{21}, T_{ij}^{12}, T_{ij}^{21}, and the nonlinear parts of K^{22} and T_{ij}^{22}. All other terms may be evaluated exactly using two-point quadrature for constant values of A_{xx} and D_{xx}.

4.2.8 Computer Implementation

The flow chart for nonlinear bending of beams is shown in Figure 4.2.4. Note that there is an outer loop on load increments (NLS=number of load steps). Except for the definition of the stiffness coefficients, much of the logic remains the same as that shown in Box 3.5.1.

The element stiffness matrix in Eq. (4.2.22) is defined by submatrices $[K^{11}]$, $[K^{12}]$, and $[K^{22}]$, and the solution vector $\{\Delta\}$ is partitioned into the axial displacement vector $\{u\}$ and vector $\{\bar{\Delta}\}$ of transverse displacements.

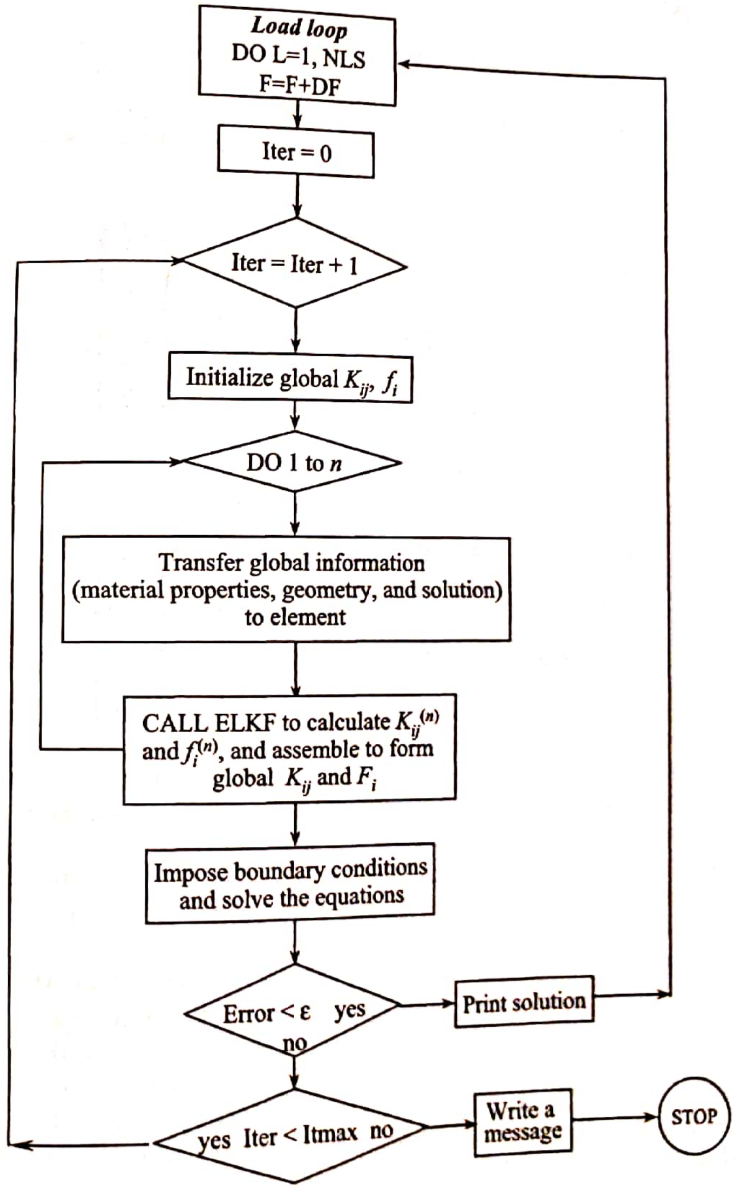

Figure 4.2.4 A computer flow chart for the nonlinear finite element analysis of beams.

In practice, it is desirable to rearrange the solution vector as

$$\{\Delta\} = \{u_1, w_1 = \bar{\Delta}_1, \theta_1 = \bar{\Delta}_2, u_2, w_2 = \bar{\Delta}_3, \theta_2 = \bar{\Delta}_4\}^T \tag{4.2.48}$$

This in turn requires rearrangement of the stiffness coefficients such that the original symmetry, if any, is preserved. For linear interpolation of $u_0(x)$ and Hermite cubic interpolation of $w_0(x)$, the submatrix $[K^{11}]$ is of the order 2×2, $[K^{12}]$ is 2×4, and $[K^{22}]$ is 4×4. Therefore, the total size of the stiffness matrix is 6×6. Thus Eq. (4.2.23) has the specific matrix form

$$\begin{bmatrix} K^{11}_{11} & K^{11}_{12} & K^{12}_{11} & K^{12}_{12} & K^{12}_{13} & K^{12}_{14} \\ K^{11}_{21} & K^{11}_{22} & K^{12}_{21} & K^{12}_{22} & K^{12}_{23} & K^{12}_{24} \\ K^{21}_{11} & K^{21}_{12} & K^{22}_{11} & K^{22}_{12} & K^{22}_{13} & K^{22}_{14} \\ K^{21}_{21} & K^{21}_{22} & K^{22}_{21} & K^{22}_{22} & K^{22}_{23} & K^{22}_{24} \\ K^{21}_{31} & K^{21}_{32} & K^{22}_{31} & K^{22}_{32} & K^{22}_{33} & K^{22}_{34} \\ K^{21}_{41} & K^{21}_{42} & K^{22}_{41} & K^{22}_{42} & K^{22}_{43} & K^{22}_{44} \end{bmatrix} \begin{Bmatrix} u^e_1 \\ u^e_2 \\ \bar{\Delta}^e_1 \\ \bar{\Delta}^e_2 \\ \bar{\Delta}^e_3 \\ \bar{\Delta}^e_4 \end{Bmatrix} = \begin{Bmatrix} F^1_1 \\ F^1_2 \\ F^2_1 \\ F^2_2 \\ F^2_3 \\ F^2_4 \end{Bmatrix} \tag{4.2.49}$$

Rearranging the equations according to the displacement vector in Eq. (4.2.48), we obtain

$$\begin{bmatrix} K^{11}_{11} & K^{12}_{11} & K^{12}_{12} & K^{11}_{12} & K^{12}_{13} & K^{12}_{14} \\ K^{21}_{11} & K^{22}_{11} & K^{22}_{12} & K^{21}_{12} & K^{22}_{13} & K^{22}_{14} \\ K^{21}_{21} & K^{22}_{21} & K^{22}_{22} & K^{21}_{22} & K^{22}_{23} & K^{22}_{24} \\ K^{11}_{21} & K^{12}_{21} & K^{12}_{22} & K^{11}_{22} & K^{12}_{23} & K^{12}_{24} \\ K^{21}_{31} & K^{22}_{31} & K^{22}_{32} & K^{21}_{32} & K^{22}_{33} & K^{22}_{34} \\ K^{21}_{41} & K^{22}_{41} & K^{22}_{42} & K^{21}_{42} & K^{22}_{43} & K^{22}_{44} \end{bmatrix} \begin{Bmatrix} u^e_1 \\ \bar{\Delta}^e_1 \\ \bar{\Delta}^e_2 \\ u^e_2 \\ \bar{\Delta}^e_3 \\ \bar{\Delta}^e_4 \end{Bmatrix} = \begin{Bmatrix} F^1_1 \\ F^2_1 \\ F^2_2 \\ F^1_2 \\ F^2_3 \\ F^2_4 \end{Bmatrix} \tag{4.2.50}$$

The computer implementation of such rearrangement of element coefficients is presented in Box 4.2.1, where NDF denotes the degrees of freedom per node (=3) and NPE the nodes per element (=2). This rearrangement is carried out after the element coefficients $[K^{11}]$, $[K^{12}]$, $[K^{22}]$, $\{F^1\} = \{0\}$, and $\{F^2\}$ are computed inside loops on Gauss quadrature. There are two loops, one for full integration and another for reduced integration.

The number of full Gauss points (NGP) is determined by the highest polynomial degree p of all integrands of the linear stiffness coefficients (recall that reduced integration is to be used for the nonlinear terms): NGP=$(p+1)/2$. For example, if linear interpolation of u_0 and Hermite cubic interpolation of w_0 is used, the integrands of the stiffness coefficients defined in Eq. (4.2.21) have the following polynomial degrees (assuming that the nonlinear terms are treated as if they are constant):

$$\begin{aligned} K^{11}_{ij} &= \text{degree of } A_{xx}, & K^{12}_{iJ} &= \text{degree of } A_{xx}, \\ K^{22(1)}_{IJ} &= \text{degree of } D^e_{xx}+2, & K^{22(2)}_{IJ} &= \text{degree of } A^e_{xx}+0 \\ F^1_i &= \text{degree of } \ f(x)+1, & F^2_I &= \text{degree of } \ q(x)+3 \end{aligned}$$

Box 4.2.1 Fortran statements to rearrange stiffness coefficients.

```
C
C     Rearranging of the element matrix coefficients for
C     the EULER-BERNOULLI beam element (EBE)
C
      II=1
      DO 200 I=1,NPE
        I0=2*I-1
        ELF(II+1)=ELF2(I0)
        ELF(II+2)=ELF2(I0+1)
        JJ=1
        DO 100 J=1,NPE
          J0=2*J-1
          ELK(II,JJ)    = ELK11(I,J)
          ELK(II,JJ+1)  = ELK12(I,J0)
          ELK(II,JJ+2)  = ELK12(I,J0+1)
          ELK(II+1,JJ)  = ELK21(I0,J)
          ELK(II+2,JJ)  = ELK21(I0+1,J)
          ELK(II+1,JJ+1) = ELK22(I0,J0)
          ELK(II+1,JJ+2) = ELK22(I0,J0+1)
          ELK(II+2,JJ+1) = ELK22(I0+1,J0)
          ELK(II+2,JJ+2) = ELK22(I0+1,J0+1)
100       JJ=NDF*J+1
200     II=NDF*I+1
```

In particular, for constant values of $AXX = A^e_{xx}$, $DXX = D^e_{xx}$, $FX = f$, and $QX = q$, we have $NGP = (3+1)/2 = 2$ (dictated by F^2_I) and the number of reduced integration points is $LGP = 1$. The full Gauss quadrature is used to evaluate $[K^{11}]$, $[K^{22(1)}]$, $\{F^1\}$, and $\{F^2\}$, whereas the reduced integration is used to evaluate $[K^{12}]$ and $[K^{22(2)}]$.

The computation of the direct stiffness coefficients and force vectors defined in Eq. (4.2.21) is straightforward. For example, we have

$$\begin{aligned} ELF1(i) &= ELF1(i) + FX * SFL(i) * CNST \\ ELF2(I) &= ELF2(I) + QX * SFH(I) * CNST \\ ELK11(i,j) &= ELK11(i,j) \\ &\quad + AXX * GDSFL(i) * GDSFL(j) * CNST \\ ELK22(I,J) &= ELK22(I,J) \\ &\quad + DXX * GDDSFH(I) * GDDSFH(J) * CNST \end{aligned}$$

in the full integration loop, and

$$\begin{aligned} ELK12(i,J) &= ELK12(i,J) + 0.5 * AXX * DW \\ &\quad * GDSFL(i) * GDSFH(J) * CNST \end{aligned}$$

$$ELK21(I,j) = ELK21(I,j) + AXX * DW * GDSFH(I) * GDSFL(j) * CNST$$

$$ELK22(I,J) = ELK22(I,J) + 0.5 * AXX * DW * DW * GDSFH(I) * GDSFH(J) * CNST$$

in the reduced integration loop. Here, $SFL(i) = \psi_i$, $SFH(I) = \phi_I$, $GDSFH(I) = \frac{d\phi_I}{dx}$, $GDDSFH(I) = \frac{d^2\phi_I}{dx^2}$, $GDSFL(i) = \frac{d\psi_i}{dx}$, and $DW = (dw_0/dx)$ for $i,j = 1,2$ and $I,J = 1,2,3,4$. Similarly, the extra terms that need to be added to the direct stiffnesses can be computed in the reduced integration loop as [see Eq. (4.2.41)]

$$TANG12(i,J) = TANG12(i,J) + 0.5 * AXX * DW * GDSFL(i) * GDSFH(J) * CNST$$

$$TANG22(I,J) = TANG22(I,J) + AXX * (DU + DW * DW) * GDSFH(I) * GDSFH(J) * CNST$$

where $DU = (du_0/dx)$.

Example 4.2.1

Consider a beam of length $L = 100$ in., 1 in. × 1 in. cross-sectional dimensions, *hinged* at both ends, made of steel ($E = 30$ msi), and subjected to uniformly distributed load of intensity q_0 lb/in. Using the symmetry about $x = L/2$, one-half of the domain is used as the computational domain. The geometric boundary conditions for the computational domain are

$$w_0(0) = u_0(L/2) = \left(\frac{dw_0}{dx}\right)_{x=\frac{L}{2}} = 0 \qquad (4.2.51)$$

The load is divided into load increments of equal size $\Delta q_0 = 1$ lb/in. A tolerance of $\epsilon = 10^{-3}$ and maximum allowable iterations of 30 (per load step) are used in the analysis. The initial solution vector is chosen to be the zero vector, so that the first iteration solution corresponds to the linear solution

$$u_0(x) = 0, \quad w_0(x) = \frac{q_0 L^4}{24 D_{xx}}\left(\frac{x}{L} - 2\frac{x^3}{L^3} + \frac{x^4}{L^4}\right) \qquad (4.2.52)$$

In particular, the center deflection is (for $q_0 = 1$)

$$w_0\left(\frac{L}{2}\right) = \frac{5 q_0 L^4}{384 D_{xx}} = 0.5208 \text{ in.} \qquad (4.2.53)$$

For the four element mesh, the linear stiffness matrix, force vector, and the global linear solution vector are given by (with the specified boundary conditions $\Delta_2 = 0$, $\Delta_{13} = 0$ and $\Delta_{15} = 0$)

$$[K^e] = 10^5 \begin{bmatrix} 24 & 0.0000 & 0.00 & -24 & 0.0000 & 0.00 \\ 0 & 0.1536 & -0.96 & 0 & -0.1536 & -0.96 \\ 0 & -0.9600 & 8.00 & 0 & 0.9600 & 4.00 \\ -24 & 0.0000 & 0.00 & 24 & 0.0000 & 0.00 \\ 0 & -0.1536 & 0.96 & 0 & 0.1536 & 0.96 \\ 0 & -0.9600 & 4.00 & 0 & 0.9600 & 8.00 \end{bmatrix}$$

$$\{F^e\} = \begin{Bmatrix} 0.000 \\ 6.250 \\ -13.021 \\ 0.000 \\ 6.250 \\ 13.021 \end{Bmatrix}, \quad \begin{Bmatrix} \Delta_3 \\ \Delta_5 \\ \Delta_6 \\ \Delta_8 \\ \Delta_9 \\ \Delta_{11} \\ \Delta_{12} \\ \Delta_{14} \end{Bmatrix} = \begin{Bmatrix} -0.01666 \\ 0.20223 \\ -0.01523 \\ 0.37109 \\ -0.01146 \\ 0.48218 \\ -0.00612 \\ 0.52083 \end{Bmatrix}$$

Table 4.2.1 contains the results of the nonlinear analysis obtained with the direct iteration procedure as well as the Newton–Raphson iteration (acceleration parameter, $\gamma = 0$). The Gauss rule $M \times N$ has the meaning that M Gauss points are used for the evaluation of linear stiffness coefficients as well as the force components, and N Gauss points are used to evaluate the nonlinear stiffness coefficients. As discussed earlier, the problem should not exhibit any nonlinearity. The correct solution (4.2.53) is predicted by the use of 2×1 Gauss rule (see the last column of Table 4.2.1). Both 4 and 8 element meshes and direct and Newton–Raphson methods predicted the same result. The 2×2 Gauss rule not only yields incorrect results, but it takes more iterations to converge.

Table 4.2.1 Finite element results for the deflections of a *hinged–hinged beam* under uniformly distributed load.

Load q_0	Direct iteration (DI) (2 × 2)		Newton–Raphson (NR) (2 × 2)		DI–NR 2 × 1
	4 elem.	8 elem.	4 elem.	8 elem.	4 and 8
1.0	0.5108 (3)*	0.5182 (3)	0.5108 (4)	0.5182 (4)	0.5208 (3)
2.0	0.9739 (5)	1.0213 (3)	0.9739 (4)	1.0213 (4)	1.0417 (3)
3.0	1.3763 (6)	1.4986 (4)	1.3764 (4)	1.4986 (4)	1.5625 (3)
4.0	1.7269 (7)	1.9451 (4)	1.7265 (4)	1.9453 (4)	2.0833 (3)
5.0	2.0356 (9)	2.3609 (5)	2.0351 (4)	2.3607 (4)	2.6042 (3)
6.0	2.3122 (11)	2.7471 (5)	2.3116 (3)	2.7467 (3)	3.1250 (3)
7.0	2.5617 (14)	3.1054 (6)	2.5630 (2)	3.1074 (2)	3.6458 (3)
8.0	2.7936 (17)	3.4418 (7)	2.7930 (2)	3.4422 (2)	4.1667 (3)
9.0	3.0049 (22)	3.7570 (7)	3.0060 (3)	3.7564 (2)	4.6875 (3)
10.0	3.2063 (29)	4.5013 (8)	3.2051 (3)	4.0523 (2)	5.2083 (3)

* Number of iterations taken to converge.

Example 4.2.2

Next, we consider the straight beam of Example 4.2.1 with (a) *pinned* ends, and (b) *clamped* ends, and under uniformly distributed transverse load. Noting the symmetry of the solution about $x = L/2$, one-half of the domain is used as the computational domain. The geometric boundary conditions for the computational domain of the two problems are

$$pinned{:}\quad u_0(0) = w_0(0) = u_0\left(\frac{L}{2}\right) = \frac{dw_0}{dx}\Big|_{x=\frac{L}{2}} = 0 \qquad (4.2.54)$$

$$clamped{:}\quad u_0(0) = w_0(0) = \frac{dw_0}{dx}\Big|_{x=0} = u_0\left(\frac{L}{2}\right) = \frac{dw_0}{dx}\Big|_{x=\frac{L}{2}} = 0 \qquad (4.2.55)$$

The load increments of $\Delta q_0 = 1.0$ lb/in., a tolerance of $\epsilon = 10^{-3}$, and maximum allowable iterations of 25 (per load step) are used in the analysis. The initial solution vector is chosen to be the zero vector. Solutions to the linear problems are

$$\textit{pinned:}\ u_0(x) = 0,\quad w_0(x) = \frac{q_0 L^4}{24D_{xx}}\frac{x^2}{L^2}\left(1 - \frac{x}{L}\right)^2 \tag{4.2.56}$$

$$\textit{clamped:}\ u_0(x) = 0,\quad w_0(x) = \frac{q_0 L^4}{24D_{xx}}\left(\frac{x}{L} - 2\frac{x^3}{L^3} + \frac{x^4}{L^4}\right) \tag{4.2.57}$$

and the maximum deflections occurs at $L/2$. For $q_0 = 1$ lb/in., $L = 100$ in., and $E = 30 \times 10^6$ psi, they are given by ($D_{xx} = EH^3/12$, $H = 1$)

$$\textit{pinned:}\ w_0\left(\frac{L}{2}\right) = \frac{5q_0L^4}{384D_{xx}} = 0.5208 \text{ in.} \tag{4.2.58}$$

$$\textit{clamped:}\ w_0\left(\frac{L}{2}\right) = \frac{q_0L^4}{384D_{xx}} = 0.1042 \text{ in.} \tag{4.2.59}$$

The linear nodal displacements obtained using four elements in half beam are

$$\begin{Bmatrix}\Delta_3\\ \Delta_5\\ \Delta_6\\ \Delta_8\\ \Delta_9\\ \Delta_{11}\\ \Delta_{12}\\ \Delta_{14}\end{Bmatrix}_{\text{pinned}} = \begin{Bmatrix}-0.01666\\ 0.20223\\ -0.01523\\ 0.37109\\ -0.11458\\ 0.48218\\ -0.00612\\ 0.52083\end{Bmatrix},\quad \begin{Bmatrix}\Delta_5\\ \Delta_6\\ \Delta_8\\ \Delta_9\\ \Delta_{11}\\ \Delta_{12}\\ \Delta_{14}\end{Bmatrix}_{\text{clamped}} = \begin{Bmatrix}0.01994\\ -0.00273\\ 0.05859\\ -0.00313\\ 0.09155\\ -0.00195\\ 0.10417\end{Bmatrix}$$

Tables 4.2.2 and 4.2.3 contain the results of the nonlinear analysis of pinned–pinned and clamped–clamped beams, respectively; the results were obtained with the Newton–Raphson iteration method. The direct iteration method did not converge even for 100 iterations per load step when $\Delta q = 1.0$. It is possible to find a value of Δq and $ITMAX$ for which one can obtain converged solutions.

Table 4.2.2 Finite element results for the deflections of a *pinned–pinned* beam under uniform load (N–R).

Load q_0	2 × 2: 4 elements	2 × 2: 8 elements	2 × 1: 4 elements	2 × 1: 8 elements
1.0	0.3669 (5)*	0.3680 (5)	0.3687 (5)	0.3685 (5)
2.0	0.5424 (4)	0.5446 (4)	0.5466 (4)	0.5457 (4)
3.0	0.6601 (3)	0.6629 (3)	0.6663 (4)	0.6645 (4)
4.0	0.7510 (3)	0.7543 (3)	0.7591 (4)	0.7564 (4)
5.0	0.8263 (3)	0.8299 (3)	0.8361 (4)	0.8324 (4)
6.0	0.8912 (3)	0.8950 (3)	0.9027 (4)	0.8979 (4)
7.0	0.9485 (3)	0.9525 (3)	0.9617 (4)	0.9558 (4)
8.0	1.0002 (3)	1.0043 (3)	1.0150 (4)	1.0080 (4)
9.0	1.0473 (3)	1.0516 (3)	1.0638 (4)	1.0557 (4)
10.0	1.0908 (3)	1.0952 (3)	1.1089 (4)	1.0997 (4)

* Number of iterations taken to converge.

There is no significant difference between the solutions obtained with the two integration rules for this problem. Figure 4.2.5 shows the load–deflection curves for the two beams. If the axial displacement degrees of freedom are suppressed (i.e. equivalent to setting $u_0 = 0$ at every point of the beam) in the nonlinear analysis of beams, the beam will behave very stiff, and the deflections experienced will be less than those shown in Tables 4.2.2 and 4.2.3 and Figure 4.2.5.

Table 4.2.3 Finite element results for the deflections of a *clamped–clamped* beam under uniform load (N–R and 2 × 1 Gauss rule).

Load q_0	Direct iteration: 4 elements	Direct iteration: 8 elements	Newton–Raphson iteration: 4 elements	Newton–Raphson iteration: 8 elements
1.0	0.1033 (3)*	0.1034 (3)	0.1034 (3)	0.1034 (3)
2.0	0.2022 (4)	0.2023 (4)	0.2022 (3)	0.2023 (3)
3.0	0.2938 (4)	0.2939 (4)	0.2939 (3)	0.2939 (3)
4.0	0.3773 (5)	0.3774 (5)	0.3773 (3)	0.3774 (3)
5.0	0.4529 (5)	0.4531 (5)	0.4528 (3)	0.4530 (3)
6.0	0.5213 (6)	0.5215 (6)	0.5214 (3)	0.5216 (3)
7.0	0.5840 (7)	0.5842 (7)	0.5839 (3)	0.5841 (3)
8.0	0.6412 (8)	0.6412 (8)	0.6413 (3)	0.6414 (3)
9.0	0.6945 (9)	0.6944 (9)	0.6943 (3)	0.6943 (3)
10.0	0.7433 (10)	0.7431 (10)	0.7435 (3)	0.7433 (3)

* Number of iterations taken to converge.

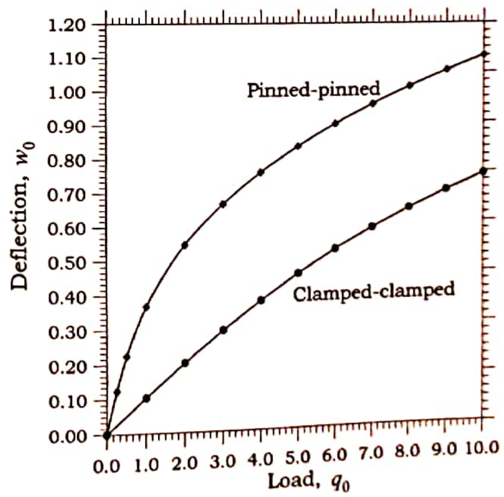

Figure 4.2.5 Load versus deflection curves.